tvst

Article

Ocular Pulse Elastography: Imaging Corneal Biomechanical Responses to Simulated Ocular Pulse Using Ultrasound

Keyton Clayson[1,2], Elias Pavlatos[1], Xueliang Pan[3], Thomas Sandwisch[1], Yanhui Ma[1], and Jun Liu[1,2,4]

[1] Department of Biomedical Engineering, The Ohio State University, Columbus, OH, USA
[2] Biophysics Interdisciplinary Group, The Ohio State University, Columbus, OH, USA
[3] Department of Biomedical Informatics, The Ohio State University, Columbus, OH, USA
[4] Department of Ophthalmology and Visual Science, The Ohio State University, Columbus, OH, USA

Correspondence: Jun Liu, 270 Bevis Hall, 1080 Carmack Road, Columbus, OH 43210, USA. e-mail: liu.314@osu.edu

Received: August 5, 2019
Accepted: November 8, 2019
Published: January 30, 2020

Keywords: corneal biomechanical properties; intraocular pressure; ocular pulse; corneal crosslinking; high frequency ultrasound elastography

Citation: Clayson K, Pavlatos E, Pan X, Sandwisch T, Ma Y, Liu J. Ocular pulse elastography: imaging corneal biomechanical responses to simulated ocular pulse using ultrasound. Trans Vis Sci Tech. 2020;9(1):5, https://doi.org/10.1167/tvst.9.1.5

Purpose: In vivo evaluation of corneal biomechanics holds the potential for improving diagnosis and management of ocular diseases. We aimed to develop an ocular pulse elastography (OPE) technique to quantify corneal strains generated by naturally occurring pulsations of the intraocular pressure (IOP) using high-frequency ultrasound.

Methods: Simulated ocular pulses were induced in whole porcine and human donor globes to investigate the effects of physiologic variations in baseline IOP, ocular pulse amplitude, and frequency on corneal strains. Ocular pulse–induced strains were measured in additional globes before and after UVA-riboflavin–induced corneal crosslinking. The central cornea in each eye was imaged with a 50-MHz ultrasound imaging system and correlation-based speckle tracking of radiofrequency data was used to calculate tissue displacements and strains.

Results: Ocular pulse–induced corneal strains followed the cyclic changes of IOP. Both baseline IOP and ocular pulse amplitude had a significant influence on strain magnitude. Variations in pulse frequency within the normal human heart rate range did not introduce detectable changes in corneal strains. A significant decrease of corneal strain, as quantified by the OPE technique, was observed after corneal crosslinking. The extent of corneal stiffening (i.e., strain reduction) seemed to correlate with the initial strain magnitude.

Conclusions: This ex vivo study demonstrated the feasibility of the OPE method to quantify corneal strains generated by IOP pulsation and detect changes associated with corneal crosslinking treatment.

Translational Relevance: Integrating in vivo measurement of IOP and ocular pulse amplitude, the OPE method may lead to a new clinical tool for safe and quick biomechanical evaluations of the cornea.

Introduction

Corneal biomechanical properties are important determinants for the shape and function of the cornea.[1] Advanced corneal imaging has significantly improved the sensitivity and specificity of screening for keratoconus[2,3]; however, early abnormalities remain difficult to diagnose. Microstructural analyses and ex vivo experimentation of keratoconic corneas suggest that corneal microstructure is altered in keratoconus leading to mechanical weakening.[4,5] A related situation is observed in patients after refractive surgery, where mechanical weakening from corneal ablation may aggravate subclinical keratoconus or innately weaker corneas leading to postsurgical corneal ectasia.[6–8]

Noninvasive methods for clinical evaluation of corneal biomechanics are thus needed to help prevent and manage these conditions.

Ultrasound elastography at 5 to 10 MHz has been adopted clinically because of its demonstrated ability to improve diagnosis of breast and liver diseases based on the added evaluation of tissue stiffness.[9–11] Elastography at higher frequencies has been used in intravascular ultrasound for analyzing atherosclerosis plaques.[12] The accessibility and small imaging depth of the cornea lends itself to the unique opportunities for very high-frequency ultrasound (i.e., ≥50 MHz) imaging[13,14] and elastography.[15–17] Moreover, the pressure inside the eye (the intraocular pressure [IOP]) fluctuates between the diastolic (baseline) and systolic (baseline + ocular pulse) pressures at each heart beat. Using these intrinsic loading and unloading cycles, we aim to develop a high-frequency ultrasound elastography method to characterize the cornea's response to the ocular pulse, termed the ocular pulse elastography (OPE) technique.[18]

The normal IOP in the human eye is about 15 mm Hg with an average ocular pulse amplitude (OPA) of about 3 mm Hg.[19] Based on reported values of corneal modulus, the compressive strains in the through-thickness direction of the cornea is estimated to be on the order of 0.1% for an average OPA.[20–22] Differentiation and quantification of tissue strains at this level have been reported previously for elastographic analysis of atherosclerotic plaque.[23,24] We have implemented similar cross-correlation based speckle tracking of ultrasound radiofrequency (RF) data, which is especially suited for precise measurement of small strains.[12] Our validation studies using controlled translation and simulated RF data at a given strain showed the ability to accurately determine axial displacements down to 0.5 μm and axial strains of 0.01% with less than 10% error.[18] These results suggest that the OPE method can provide sufficient sensitivity and accuracy to quantify corneal strains induced by the ocular pulse and potentially offer a tool for the in vivo evaluation of corneal biomechanics.

In this study, we measured corneal strains in response to simulated ocular pulses in ex vivo porcine and human donor globes while varying the parameters of IOP (namely, the baseline IOP, the OPA, and the pulse frequency) within their respective physiologic ranges. Our goal was to determine the influence of these parameters on corneal strains measured by the OPE technique. These results will serve as a basis for building algorithms or models to interpret and analyze future in vivo data from human subjects measured at various combinations of these parameters. We also evaluated the feasibility of detecting and quantifying corneal biomechanical changes after corneal crosslinking (CXL)[25] to evaluate the sensitivity of the OPE technique in detecting clinically relevant corneal stiffening.

Methods

Porcine and Human Globe Preparation

Porcine whole globes (one per animal) were obtained from a US Department of Agriculture–approved abattoir under Hazard Analysis and Critical Control Point guidelines (SiouxPreme Packing Co., Sioux City, IA), transported and stored at 4°C in 0.9% saline, and tested within 72 hours postmortem. Human donor globes were obtained from the Lions Eye Bank of West Central Ohio (Dayton, OH), transported at 4°C in a sealed moist container, and tested within 48 hours postmortem. All donor eyes had no known history of ocular trauma, ocular surgery, or corneal diseases. The age span of the donors was 20 to 78 years old.

Owing to the substantial corneal swelling observed in human donor eyes upon arrival at the laboratory (e.g., posterior corneal folds as seen on ultrasound scans), corneal deswelling was performed by immersing the globes in 3.5% poloxamer-188 solution in 0.9% saline (Kolliphor 188, Sigma Aldrich, MO) at 4°C,[26,27] with the IOP being maintained near 15 mm Hg and the anterior chamber being perfused with the same solution, for at least 18 hours until corneal thickness stabilized. The globes remained immersed in the same solution during testing.

All globes were secured to a custom-built eye holder during testing using two 20G spinal needles inserted at the equator of the eye, as shown in Figure 1a. A 20G needle was inserted into the anterior chamber through the limbus along the superior-inferior axis and connected to a fluid column to control baseline IOP and a programmable syringe pump (PhD Ultra, Harvard Apparatus, Boston, MA) to simulate ocular pulses. Another 20G needle was inserted along the same axis and connected to a pressure sensor (P75 venous pressure transducer, Harvard Apparatus) to monitor IOP during experimentation. Before testing, all globes were preconditioned with 25 pressure cycles from 5 to 30 mm Hg and equilibrated at 15 mm Hg at room temperature for 30 minutes.

Simulated Ocular Pulse Cycles

Ocular pulses at different baseline IOP, OPA, and frequency were simulated and the cornea's

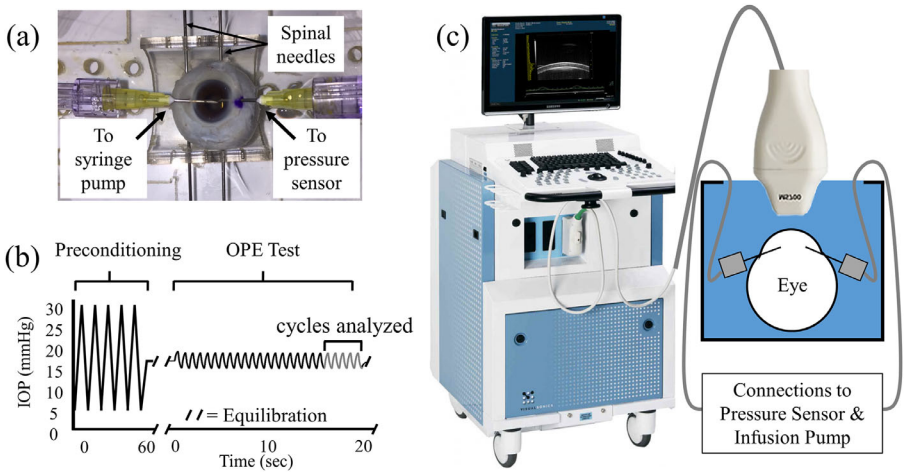

Figure 1. (a) Mounting of a human donor globe for pressure control and monitoring. (b) Representative OPE test protocol. (c) Overall experimental setup using the Vevo 2100 ultrasound imaging system with an MS700 probe.

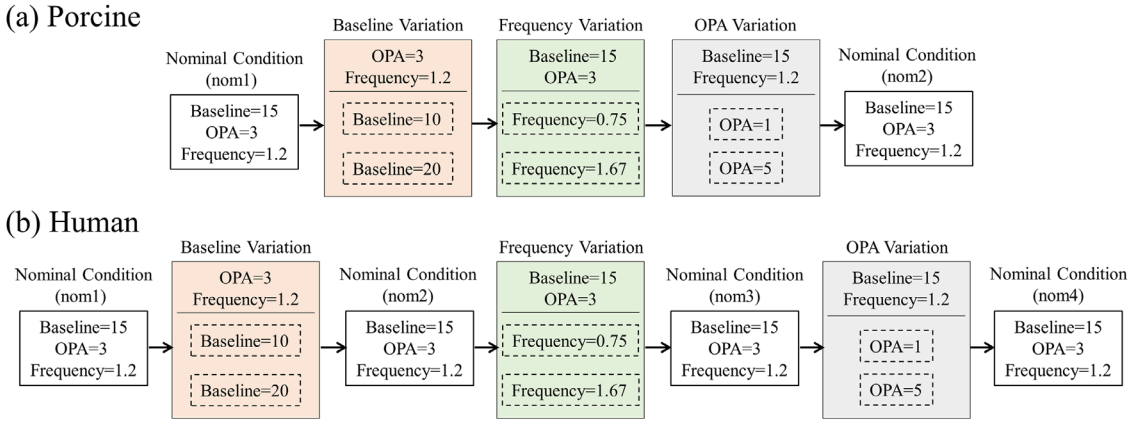

Figure 2. Flow chart of the order of 7 different testing conditions in (a) porcine and (b) human donor eyes, to evaluate the influence of baseline IOP, OPA, and frequency. The parameters were varied one at a time from nominal conditions (i.e., base = 15 mm Hg, OPA = 3 mm Hg, frequency = 1.2 Hz) to cover the normal ranges seen in humans. In porcine eyes, the nominal condition was performed at the beginning (nom1) and repeated once at the end (nom2), while in human donor eyes the nominal condition was performed at the beginning (nom1) and repeated after each group of testing (nom2, nom3, nom4). Base, baseline IOP; freq, simulated ocular pulse frequency; OPA, simulated OPA.

response was measured in the same eye under different combinations of these parameters. The nominal condition has parameter values close to the population mean, that is, a baseline IOP of 15 mm Hg, an OPA of 3 mm Hg, and a frequency of 1.2 Hz (corresponding with a heart rate of 72 beats per minute). The parameters were varied one at a time within their respective physiologic ranges: that is, baseline IOP to 10 or 20 mm Hg, OPA to 1 or 5 mm Hg, and frequency to 0.75 or 1.67 Hz. The globes were equilibrated for 15 minutes after a change in baseline IOP; tests at the same baseline IOP were performed immediately after the previous test. Our previous study showed very high repeatability of the OPE measurements with an intraclass correlation of 0.98[18] when experiments under the same condition were repeated within minutes in the same eye. Owing to the much longer experimental time (about 2 hours) in completing multiple measurements under different conditions, some changes in tissue properties (e.g., hydration level) may occur in the postmortem eyes and thus the same nominal condition test was repeated at different time points to evaluate if there were tissue changes. Ten porcine and 14 human donor eyes were used for evaluating corneal strains under different IOP parameters. The testing protocols for porcine and human donor eyes are presented in Figure 2. The same nominal condition was tested twice in the porcine eyes (nom1 and nom2 in Fig. 2a) and four times in the human donor eyes (nom1, nom2, nom3, and nom4 in Fig. 2b).

High-Frequency Ultrasound Elastography

For each testing condition, the globe underwent 25 consecutive ocular pulse cycles (Fig. 1b) and the first 20 cycles preconditioned the cornea for the specific loading parameters of that test. During the last five cycles of each test, ultrasound RF data of the central 5.7 mm of cornea were acquired by a 50- MHz ultrasound probe (MS700) of the Vevo 2100 ultrasound imaging system (FUJIFILM VisualSonics, Toronto, Ontario, Canada) along the nasal–temporal meridian at a frame rate of 128 frames per second (Figs. 1b, c).

The displacement vector field was calculated using an ultrasound speckle tracking algorithm as described previously.[18,28] Briefly, a region of interest was defined in the first image of each cycle at the baseline IOP (i.e., the reference image). The RF data within the region of interest was divided into approximately 60 to 90 kernels each containing 151 × 41 pixels (axial × lateral), or about 225 × 780 μm in size. A 50% kernel overlap was adopted for optimal tradeoff between signal-to-noise ratio and spatial resolution of the strain map.[28] To compute the displacement at each kernel, normalized cross-correlation was used to identify the new location of each kernel in the next consecutive image (i.e., the deformed image) within a predefined search window. Spline interpolation of the correlation coefficients was used to achieve displacement sensitivity at the subpixel level. Displacements and strains were calculated separately for each of the five cycles.

Both axial and lateral displacements were calculated at each kernel. Owing to the higher accuracy of axial displacements,[18] axial strains calculated from axial displacements were reported in the present study. Because of the small thickness of the cornea, axial strains were calculated using a robust fit multilinear function performed on entire axial columns of displacement data (regress in MATLAB, r2018a, The Mathworks, Inc., Natick, MA). The robust fit function better decreases outlier effects of the boundary kernels as compared with traditional least squares estimation.[28] Displacement maps were generated at the level of kernels, and strain maps were interpolated at each pixel and smoothed to visualize the spatial distribution of strains.

Corneal Crosslinking

Eight porcine and six human donor eyes were used to evaluate the changes in corneal strains after a standard CXL procedure was performed. The epithelium in all corneas was gently removed by scraping with a blunt scalpel blade. Globes were preconditioned with 25 pressure cycles from 5 to 30 mm Hg and stabilized at 15 mm Hg for at least 10 minutes, after which an ocular pulse test at the nominal condition was performed (the "before" case). The cornea was then subjected to UVA-riboflavin treatment with IOP maintained at 15 mm Hg. The cornea was pretreated with riboflavin solution (VibeX Rapid, Avedro, Waltham, MA; 0.12% riboflavin) at 2-minute intervals for 10 minutes, then irradiated with UVA radiation (Vega CBM-X-Linker, CSO Italia, Florence, Italy; 360 nm, 3 mW/cm^2 irradiance) for 30 minutes with continuous reapplication of riboflavin solution at 5-minute intervals. After treatment, the globe was stabilized in an immersion solution for at least 10 minutes and an additional ocular pulse test at the nominal condition was performed (the "after" case).

Statistical Analysis

All data analysis results were conducted using SAS 9.4 (SAS Institute Inc, Cary, NC). Corneal axial strains were summarized using mean and standard deviation. Corneal axial strains for each combination of IOP parameters were compared using linear mixed models with repeated measures. Corneal strains before and after CXL were compared using paired *t*-tests. Pearson correlation coefficients were calculated to evaluate the association between the initial strain and strain reduction after CXL in the combined dataset including both porcine and human eyes.

Results

Axial Displacements and Strains

Maps of correlation coefficients and axial displacements of each kernel at peak pressure were generated. In all tested eyes, the average correlation coefficient was more than 0.9, suggesting excellent tracking (Fig. 3a). Maps of relative displacements (subtracting the overall mean) were used to better visualize displacement gradient (Fig. 3b). In both porcine and human donor corneas, a through-thickness gradient was observed, with smaller relative displacements in the anterior cornea and larger relative displacements in the posterior cornea resulting in compressive strains (Fig. 3c).

In both porcine and human donor eyes, strains followed the cyclic changes in IOP (Fig. 3d). Four human donor eyes showed greater strain variance under the four nominal conditions, with coefficients

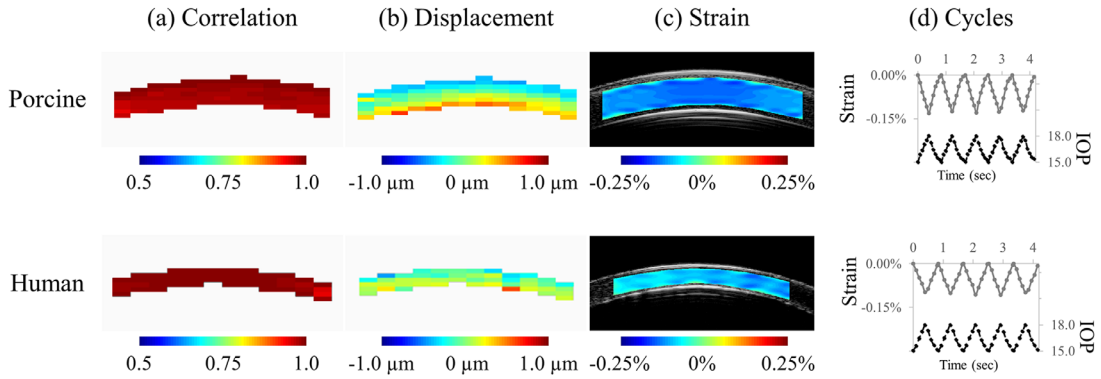

Figure 3. Representative maps of (a) correlation coefficients, (b) displacements, and (c) strains measured at the peak pressure of the nominal condition (baseline IOP = 15 mm Hg, OPA = 3 mm Hg, frequency = 1.2 Hz), in a porcine and a human donor eye. (d) Cyclic strains following changes in IOP.

of variance (COV) of 38%, 59%, 76%, and 138%, as compared with the remaining 10 donor eyes with COVs from 4% to 27% (mean 16.3% ± 7.5%) and the 10 porcine eyes with COVs from 1% to 19% (7.3% ± 5.0%). Among the four human eyes, two had strains close to or less than 0.01%, our previously determined accuracy threshold[18]; one had positive strains in one-half of the measured cross-section indicating significant swelling; and the last one had unrepeatable nominal response (COV of 38%) for an unidentified reason. Those four eyes were excluded from further analyses owing to their nonrepeated nominal responses. The average axial strains at peak pressure under the nominal condition in the remaining 10 human donor eyes was –0.080% ± 0.025%, significantly smaller ($P < 0.004$, two-sample t-test) than that in the tested porcine eyes (–0.120% ± 0.027%; n = 10).

Influence of Baseline IOP, OPA, and Frequency

In porcine eyes, the measured corneal strains under different testing conditions were significantly different based on the analysis using a linear mixed model ($P < 0.001$, linear mixed models). A small but significant difference between the two nominal tests were observed (nom1 = –0.126% ± 0.029%; nom2 = –0.114% ± 0.027%; $P < 0.001$, paired t-test). When compared with the nominal average (–0.120% ± 0.027%), decreasing the OPA to 1 mm Hg (–0.040% ± 0.011%) and increasing the baseline IOP to 20 mm Hg (–0.072% ± 0.019%) resulted in significant decreases in corneal strain (both $P < 0.001$), whereas increasing the OPA to 5 mm Hg (–0.186% ± 0.044%) and decreasing the baseline IOP to 10 mm Hg (–0.350% ± 0.137%) resulted in significant increases in corneal strain (both $P < 0.005$). Changes in frequency to 0.75 Hz (–0.124% ± 0.026%) or 1.67 Hz (–0.116% ± 0.026%) did not result in significant changes in strains from the nominal conditions (both $P > 0.05$).

In human eyes, the measured corneal strains under different testing conditions were also significantly different based on the analysis using a linear mixed model ($P < 0.001$). The strains under nominal conditions were not significantly different (nom1 = –0.084% ± 0.026%; nom2 = –0.080% ± 0.031%; nom3 = –0.074% ± 0.037%; nom4 = –0.082% ± 0.031%; n = 10; all $P > 0.05$, paired t-tests). When compared with the nominal average (–0.080% ± 0.025%), decreasing the OPA to 1 mm Hg (–0.028% ± 0.010%) and increasing the baseline IOP to 20 mm Hg (–0.036% ± 0.019%) resulted in significant decreases in corneal strain (both $P < 0.001$), whereas increasing the OPA to 5 mm Hg (–0.111% ± 0.048%) and decreasing the baseline IOP to 10 mm Hg (–0.168% ± 0.107%) resulted in significant increases in corneal strain (both $P < 0.005$). Changes in frequency to 0.75 Hz (–0.075% ± 0.034%) or 1.67 Hz (–0.072% ± 0.034%) did not result in significant changes in strains from the nominal conditions (both $P > 0.05$).

Representative corneal strain maps and average response under different testing conditions are shown in Figure 4. The central corneal thickness (CCT) in each eye was determined using the built-in software of the Vevo 2100 ultrasound imaging system following a previously reported method.[29] The average CCT in human donor eyes was 611 ± 56 µm (range, 511–700 µm), somewhat higher than the reported population average of 544 ± 34 µm for in vivo CCT,[30] indicating slight overhydration. The average porcine CCT was 983 ± 52 µm, which is comparable with our previously reported results of 988 ± 46 µm in porcine eyes from the same source.[27]

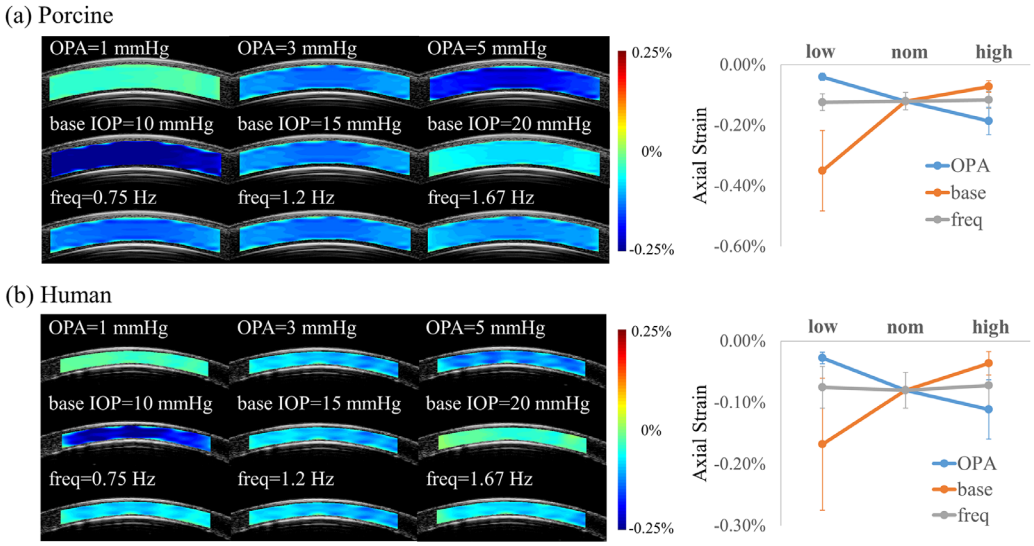

Figure 4. Representative corneal axial strain maps and average strain response of simulated ocular pulse cycles in (a) porcine and (b) human corneas. base, baseline IOP; freq, simulated ocular pulse frequency; high, highest value of one of the parameters (baseline IOP = 20 mm Hg, OPA = 5 mm Hg, or frequency = 1.67 Hz); low, lowest value of one of the parameters (baseline IOP = 10 mm Hg, OPA = 1 mm Hg, or frequency = 0.75 Hz); nom, nominal condition (baseline IOP = 15 mm Hg, OPA = 3 mm Hg, and frequency = 1.2 Hz); OPA, simulated OPA.

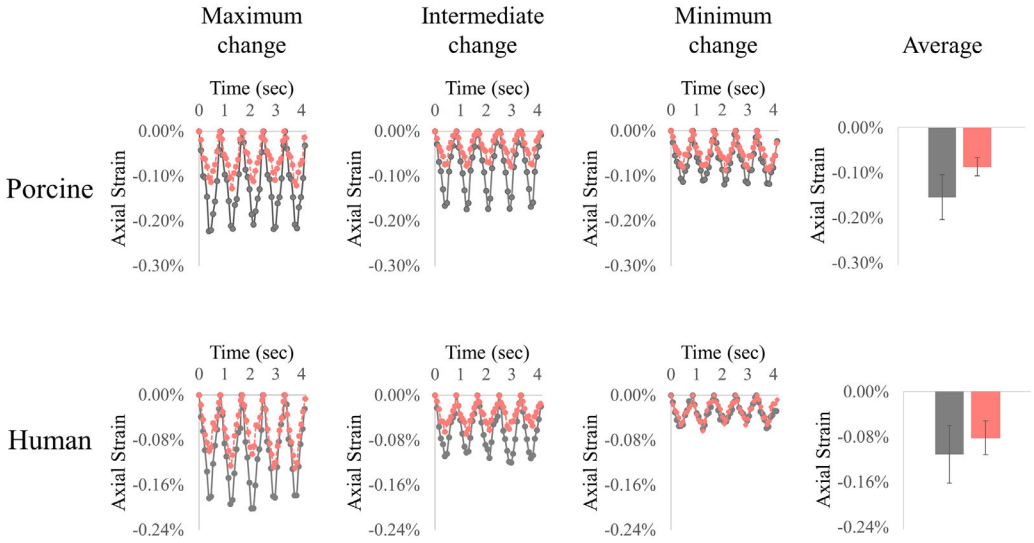

Figure 5. Representative strains before (black) and after (red) CXL treatment in porcine and human corneas. The level of strain reduction was different in different eyes, and the cases from left to right show examples of substantial strain reduction to small/minimal strain reduction. Average strain before and after CXL in the two groups are shown on the right.

Effect of CXL

Corneal strains at peak pressure were significantly reduced after CXL in both porcine (n = 8; –0.154% ± 0.045% before vs. –0.086% ± 0.023% after; $P < 0.001$; Fig. 5a) and human (n = 6; –0.111% ± 0.051% before vs. –0.081% ± 0.034% after; $P = 0.038$; Fig. 5b) corneas. The initial strain magnitudes varied considerably in both porcine and human donor globes (ranging from 0.11% to 0.22% in porcine globes and 0.06% to 0.19% in human globes). Explorative correlation analyses showed that the change in strain magnitudes was positively correlated with the initial strain magnitude, with Pearson correlation coefficients R = 0.902 in porcine eyes (n = 8; $P = 0.002$) and R = 0.818 in human eyes (n = 6; $P = 0.047$). When porcine and human donor data were combined, the overall correlation was 0.880 (n = 14; $P < 0.001$; Fig. 6).

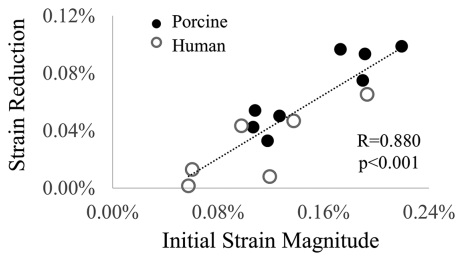

Figure 6. Higher initial strain magnitude was associated with larger strain reduction after CXL.

Discussion

In this study, we used a high-frequency ultrasound speckle tracking technique to measure corneal strains generated by simulated ocular pulses in donor and animal eyes. Changes in baseline IOP and OPA resulted in significant changes in corneal strain magnitudes, whereas frequency did not. CXL treatment resulted in detectable decreases in corneal strains that seemed to be correlated with the initial strain. These results indicate that the OPE method may provide a sensitive and accurate method to quantify corneal biomechanical responses to the eye's intrinsic pressure pulse.

High-frequency ultrasound examination has the spatial and temporal resolution for capturing small, rapid changes in tissue displacements and strains. We implemented speckle tracking in RF data with interpolation of correlation coefficients, resulting in displacement sensitivity approaching tens of nanometers.[18,31,32] This high sensitivity enabled the detection of the spatial gradient of displacement despite a small range of magnitudes (i.e., within a few micrometers) (Fig. 3). Our previous studies on simulated RF data showed satisfactory accuracy for axial strains of greater than 0.01%.[18] The magnitude of the ocular pulse–induced axial strain was over this threshold in all tested porcine eyes and 12 of the 14 tested human donor eyes. Although it may be desirable to accurately measure strains smaller than 0.01%, clinically it is more important to quantify larger-than-normal strains (i.e., higher compliance), because corneal conditions such as keratoconus and postsurgical ectasia are associated with mechanical weakening and, thus, greater deformation. It is also perceivable that controlled IOP elevation larger than the ocular pulse may be temporarily applied to induce larger corneal deformation.

The baseline IOP had a significant effect on corneal strains in both porcine and human corneas (Fig. 4). This difference can be explained by the known nonlinear mechanical behavior of the cornea,[33,34] which manifests as a more compliant response at lower IOP and a stiffer response at higher IOP. It is noted that the effect of baseline IOP on ocular pulse–induced corneal strains was not linear (Fig. 4), and future studies are needed to further characterize this response to develop normalization algorithms for this parameter. OPA also had a significant effect on corneal strain, which is readily expected, because a larger loading pressure will generate a larger deformation. The strains for an OPA of 1 mm Hg were small in most tested donor eyes, which may present a challenge for accurate quantification; however, it has been shown that an OPA of 1 mm Hg or less is uncommon in humans.[19] The effect of OPA seemed to be almost linear, suggesting the potential use of a simple proportionality factor to normalize this parameter. These results also demonstrated the sensitivity of the OPE method, because it consistently and robustly detected the expected differences in corneal responses owing to the physiologic variations in OPA and baseline IOP.

Interestingly, changes in frequency from 0.75 Hz to 1.67 Hz did not introduce significant changes in the magnitudes of corneal strains (Fig. 4). This finding may seem to be contradictory to what would be expected from the known viscoelasticity of the cornea,[35,36] because a viscoelastic material behaves differently to load applied at different speeds. Tensile testing of corneal strips has shown that the faster the strain rate (i.e., the speed of applying load), the stiffer the cornea behaves.[20] The results in the current study can be explained by the following two observations. First, only a small frequency range (0.75–1.67 Hz) corresponding with the physiologic range of heart rate (about 45–100 beats per minute) was tested in the current study, whereas the strain rate dependence observed in previous studies used rates across orders of magnitude.[21] Second, the ocular pulse was superimposed on a much larger preloading (i.e., the baseline IOP). Previous dynamic mechanical testing on corneal strips by superimposing a small sinusoidal dynamic loading onto a prestretched cornea has reported that corneal dynamic modulus was independent of frequency within 3.5 to 110.0 Hz.[37] Our results were consistent with this finding, indicating that the contributions of the viscous component were small for the dynamic inputs superimposed on a cornea prestrained by the baseline IOP. Our current experimental system does not allow precise determination of the phase lag between IOP and corneal strain, but it may be evaluated in future studies to better understand the viscoelastic response of the cornea and the relationship between the spectral parameters of IOP and corneal strains.[38]

A significant decrease in corneal strains was observed after CXL treatment in both porcine and human corneas (Fig. 5). Given that all testing was performed at the nominal condition, strain reduction

indicates stiffening, confirming the effect of CXL in increasing the mechanical stiffness of the cornea.[39] Quantitatively, corneal axial strains decreased by 43% in porcine eyes and 24% in human donor eyes after CXL, consistent with the reported ranges from previous inflation studies.[40,41] On average, porcine corneas had more compliant response (larger strains) as compared with human corneas, also consistent with previous observations.[42,43]

Our explorative correlation analysis of the CXL-treated corneas indicated that the initial stiffness may be an important factor affecting the extent of the stiffening; that is, the same CXL procedure may be more effective on a more compliant cornea than a stiffer cornea (Fig. 6). This may explain the decreased efficacy of CXL treatment in patients more than 26 years old[44,45]; corneal stiffness increases with advancing age, likely owing to an increase in glycation-mediated collagen crosslinking.[46] A method to map and quantify corneal stiffness before CXL, such as the OPE technique presented in this work, may to help predict the extent of stiffening that can be achieved.

In vivo biomechanical characterization of the cornea is an important goal of ongoing research.[15,47–54] The present study in ex vivo eyes aimed to establish the feasibility of using high-frequency ultrasound elastography to measure the cornea's response to the intrinsic ocular pulse without applying external forces. The maximum acoustic intensity (spatial peak, temporal average) of our ultrasound imaging system is 11 mW/cm^2 and the maximum mechanical index is 0.4. Our ongoing in vivo measurements in human volunteers have shown that only 10% power is needed owing to the much greater echogenicity of the human cornea in vivo. The acoustic energy needed is thus within the US Food and Drug Administration–approved threshold for ophthalmic ultrasound.[55] The patient examination protocol is similar to what is experienced during clinical ophthalmic ultrasound examination and the data acquisition can be completed within minutes. Preliminary analysis has shown displacement cycles of the same frequency as the cardiac cycles, and compressive axial strains of similar order of magnitudes as observed in donor eyes (Liu J, et al. *IOVS*. 2019;60:ARVO E-Abstract 6800).

Eye motion during in vivo measurements could affect continuous speckle tracking of a specific corneal plane between consecutive scanning frames. Our previous results showed that speckle tracking remained successful for up to 32 µm of out-of-plane movement.[18] Some involuntary eye motions, such as microsaccades, drift, and tremor,[56] could introduce noise and strain artefacts. Work is ongoing to analyze eye motion–related strain artifacts and develop methods to minimize such noise.

There are a few limitations in the present study. Corneal hydration has been shown to significantly influence mechanical response.[22,57,58] Despite our effort to control hydration, there was a small yet significant difference between the two nominal tests in the porcine globes, possibly owing to slight changes in hydration. Nonetheless, the strain difference was minimal (from 0.126% to 0.114%), substantially smaller than the observed difference between testing conditions and, therefore, should not alter the overall outcome of the study. Corneal thickness change during CXL in this study (data not shown) was consistent with other reports.[59,60] Second, the current study only evaluated axial strains. For the central cornea, the axial strain should be very close to the radial strain in the through-thickness direction. Although previous studies have shown a correlation between the in-plane and through-thickness responses,[41] future work is needed to improve the lateral analysis to better characterize the in-plane response. Third, the influence of the baseline IOP and OPA were clearly demonstrated in the present study, but a method to obtain biomechanical evaluations of the cornea independent of IOP remains to be developed. We previously proposed a method to derive a corneal stiffness index using analytical models.[18] Improved models that incorporate clinically measurable IOP and corneal parameters are being developed.

In summary, we have developed and demonstrated the feasibility of the OPE technique to precisely quantify corneal strains in response to the ocular pulse using high-frequency ultrasound speckle tracking. An understanding of how the loading parameters affect corneal strains will help to build models to derive intrinsic tissue properties from the strain response. Significant strain reduction after CXL treatment as quantified by OPE suggested that this technique may potentially help assess treatment efficacy and guide therapeutic planning. Work is ongoing to translate this technique to a clinical tool for in vivo corneal biomechanical evaluation to improve diagnosis and decision making in the treatment of corneal diseases.

Acknowledgments

Supported by NIH grant R01EY025358.

Disclosure: **K. Clayson,** None; **E. Pavlatos,** None; **X. Pan,** None; **T. Sandwisch,** None; **Y. Ma,** None; **J. Liu,** None

References

1. Ruberti JW, Sinha Roy A, Roberts CJ. Corneal biomechanics and biomaterials. *Annu Rev Biomed Eng*. 2011;13:269–295.
2. Belin MW, Villavicencio OF, Ambrósio RR. Tomographic parameters for the detection of keratoconus: suggestions for screening and treatment parameters. *Eye Contact Lens*. 2014;40:326–330.
3. Swartz T, Marten L, Wang M. Measuring the cornea: the latest developments in corneal topography. *Curr Opin Ophthalmol*. 2007;18:325–333.
4. Meek KM, Tuft SJ, Huang Y, et al. Changes in collagen orientation and distribution in keratoconus corneas. *Invest Ophthalmol Vis Sci*. 2005;46:1948.
5. Andreassen TT, Hjorth Simonsen A, Oxlund H. Biomechanical properties of keratoconus and normal corneas. *Exp Eye Res*. 1980;31:435–441.
6. Randleman JB, Woodward M, Lynn MJ, Stulting RD. Risk assessment for ectasia after corneal refractive surgery. *Ophthalmology*. 2008;115:3–10.e4.
7. Wolle MA, Randleman JB, Woodward MA. Complications of refractive surgery: ectasia after refractive surgery. *Int Ophthalmol Clin*. 2016;56:127–139.
8. Ambrósio R, Jr, Nogueira LP, Caldas DL, et al. Evaluation of corneal shape and biomechanics before LASIK. *Int Ophthalmol Clin*. 2011;51:11–38.
9. Barr RG. Sonographic breast elastography: a primer. *J Ultrasound Med*. 2012;31:773–783.
10. Ferraioli G, Wong VW, Castera L, et al. Liver ultrasound elastography: an update to the World Federation for Ultrasound in Medicine and Biology guidelines and recommendations. *Ultrasound Med Biol*. 2018;44:2419–2440.
11. Frulio N, Trillaud H. Ultrasound elastography in liver. *Diagn Interv Imaging*. 2013;94:515–534.
12. de Korte CL, van der Steen Anton FW. Intravascular ultrasound elastography: an overview. *Ultrasonics*. 2002;40:859–865.
13. Reinstein DZ, Yap TE, Archer TJ, Gobbe M, Silverman RH. Comparison of corneal epithelial thickness measurement between Fourier-domain OCT and very high-frequency digital ultrasound. *J Refract Surg*. 2015;31:438–445.
14. Silverman RH, Urs R, Roychoudhury A, Archer TJ, Gobbe M, Reinstein DZ. Epithelial remodeling as basis for machine-based identification of keratoconus. *Invest Ophthalmol Vis Sci*. 2014;55:1580–1587.
15. Hollman K, Shtein RM, Tripathy S, Kim K. Using an ultrasound elasticity microscope to map three-dimensional strain in a porcine cornea. *Ultrasound Med Biol*. 2013;39:1451–1459.
16. Osapoetra LO, Watson DM, McAleavey SA. Intraocular pressure–dependent corneal elasticity measurement using high-frequency ultrasound. *Ultrasonic Imaging*. 2019;41:251.
17. Qian X, Ma T, Shih C, et al. Ultrasonic Microelastography to assess biomechanical properties of the cornea. *IEEE Trans Biomed Eng*. 2019;66:647–655.
18. Pavlatos E, Chen H, Clayson K, Pan X, Liu J. Imaging corneal biomechanical responses to ocular pulse using high-frequency ultrasound. *IEEE Trans Med Imaging*. 2018;37:663–670.
19. Kaufmann C, Bachmann LM, Robert YC, Thiel MA. Ocular pulse amplitude in healthy subjects as measured by dynamic contour tonometry. *Arch Ophthalmol*. 2006;124:1104–1108.
20. Elsheikh A, Anderson K. Comparative study of corneal strip extensometry and inflation tests. *J R Soc Interface*. 2005;2:177–185.
21. Elsheikh A, Wang D, Pye D. Determination of the modulus of elasticity of the human cornea. *J Refract Surg*. 2007;23:808–818.
22. Hatami-Marbini H, Etebu E. Hydration dependent biomechanical properties of the corneal stroma. *Exp Eye Res*. 2013;116:47–54.
23. de Korte CL, Pasterkamp G, van der Steen Anton FW, Woutman HA, Bom N. Characterization of plaque components with intravascular ultrasound elastography in human femoral and coronary arteries in vitro. *Circulation (Baltimore)*. 2000;102:617–623.
24. de Korte CL, Carlier SG, Mastik F, et al. Morphological and mechanical information of coronary arteries obtained with intravascular elastography; feasibility study in vivo. *Eur Heart J*. 2002;23:405–413.
25. Wollensak G, Spoerl E, Seiler T. Riboflavin/ultraviolet-a–induced collagen crosslinking for the treatment of keratoconus. *Am J Ophthalmol*. 2003;135:620–627.
26. Zhao M, Thuret G, Piselli S, et al. Use of poloxamers for deswelling of organ-cultured corneas. *Invest Ophthalmol Vis Sci*. 2008;49:550–559.
27. Clayson K, Sandwisch T, Ma Y, Pavlatos E, Pan X, Liu J. Corneal hydration control during ex vivo experimentation using poloxamers. *Curr Eye Res*. 2019;18:1–7.
28. Tang J, Liu J. Ultrasonic measurement of scleral cross-sectional strains during elevations of intraocular pressure: method validation and initial

results in posterior porcine sclera. *J Biomech Eng*. 2012;134:091007.
29. Palko JR, Pan X, Liu J. Dynamic testing of regional viscoelastic behavior of canine sclera. *Exp Eye Res*. 2011;93:825–832.
30. Doughty MJ, Zaman ML. Human corneal thickness and its impact on intraocular pressure measures: a review and meta-analysis approach. *Surv Ophthalmol*. 2000;44:367–408.
31. Ma Y, Pavlatos E, Clayson K, et al. Mechanical deformation of human optic nerve head and peripapillary tissue in response to acute IOP elevation. *Invest Ophthalmol Vis Sci*. 2019;60:913–920.
32. Hansen HHG, Lopata RGP, Idzenga T, de Korte CL. Full 2D displacement vector and strain tensor estimation for superficial tissue using beam-steered ultrasound imaging. *Phys Med Biol*. 2010;55:3201–3218.
33. Clayson K, Pan X, Pavlatos E, et al. Corneoscleral stiffening increases IOP spike magnitudes during rapid microvolumetric change in the eye. *Exp Eye Res*. 2017;165:29–34.
34. Woo SL, Kobayashi AS, Schlegel WA, Lawrence C. Nonlinear material properties of intact cornea and sclera. *Exp Eye Res*. 1972;14:29–39.
35. Boyce BL, Jones RE, Nguyen TD, Grazier JM. Stress-controlled viscoelastic tensile response of bovine cornea. *J Biomech*. 2006;40:2367–2376.
36. Elsheikh A, Wang D, Rama P, Campanelli M, Garway-Heath D. Experimental assessment of human corneal hysteresis. *Curr Eye Res*. 2008;33:205–213.
37. Kaplan D, Bettelheim FA. Dynamic rheotopical behavior of isolated bovine cornea. *Biophys J*. 1972;12:1630–1641.
38. Rogala MM, Danielewska ME, Antończyk A, et al. In-vivo corneal pulsation in relation to in-vivo intraocular pressure and corneal biomechanics assessed in-vitro. An animal pilot study. *Exp Eye Res*. 2017;162:27–36.
39. Wollensak G, Spoerl E, Seiler T. Stress-strain measurements of human and porcine corneas after riboflavin–ultraviolet-A-induced cross-linking. *J Cataract Refract Surg*. 2003;29:1780–1785.
40. Kling S, Remon L, Pérez-Escudero A, Merayo-Lloves J, Marcos S. Corneal biomechanical changes after collagen cross-linking from porcine eye inflation experiments. *Invest Ophthalmol Vis Sci*. 2010;51:3961.
41. Palko JR, Tang J, Cruz Perez B, Pan X, Liu J. Spatially heterogeneous corneal mechanical responses before and after riboflavin–ultraviolet-A crosslinking. *J Cataract Refract Surg*. 2014;40:1021–1031.
42. Elsheikh A, Alhasso D, Rama P. Biomechanical properties of human and porcine corneas. *Exp Eye Res*. 2008;86:783–790.
43. Zeng Y, Yang J, Huang K, Lee Z, Lee X. A comparison of biomechanical properties between human and porcine cornea. *J Biomech*. 2001;34:533–537.
44. Caporossi A, Mazzotta C, Baiocchi S, Caporossi T. Long-term results of riboflavin ultraviolet a corneal collagen cross-linking for keratoconus in Italy: the Siena Eye Cross Study. *Am J Ophthalmol*. 2010;149:585–593.
45. Caporossi A, Mazzotta C, Baiocchi S, Caporossi T, Denaro R. Age-related long-term functional results after riboflavin UV A corneal cross-linking. *J Ophthalmol*. 2011;2011:608041.
46. Knox Cartwright NE, Tyrer JR, Marshall J. Age-related differences in the elasticity of the human cornea. *Invest Ophthalmol Vis Sci*. 2011;52:4324–4329.
47. Ford MR, Roy AS, Rollins AM, Dupps WJ. Serial biomechanical comparison of edematous, normal, and collagen crosslinked human donor corneas using optical coherence elastography. *J Cataract Refract Surg*. 2014;40:1041–1047.
48. Han Z, Li J, Singh M, et al. Optical coherence elastography assessment of corneal viscoelasticity with a modified Rayleigh-Lamb wave model. *J Mech Behav Biomed Mater*. 2017;66:87–94.
49. Luce DA. Determining in vivo biomechanical properties of the cornea with an ocular response analyzer. *J Cataract Refract Surg*. 2005;31:156–162.
50. Scarcelli G, Besner S, Pineda R, Yun SH. Biomechanical characterization of keratoconus corneas ex vivo with Brillouin microscopy. *Invest Ophthalmol Vis Sci*. 2014;55:4490–4495.
51. Vinciguerra R, Elsheikh A, Roberts CJ, et al. Influence of pachymetry and intraocular pressure on dynamic corneal response parameters in healthy patients. *J Refract Surg*. 2016;32:550–561.
52. Mikula E, Hollman K, Chai D, Jester JV, Juhasz T. Measurement of corneal elasticity with an acoustic radiation force elasticity microscope. *Ultrasound Med Biol*. 2014;40:1671–1679.
53. Nguyen T, Aubry J, Touboul D, et al. Monitoring of cornea elastic properties changes during UV-A/riboflavin-induced corneal collagen cross-linking using supersonic shear wave imaging: a pilot study. *Invest Ophthalmol Vis Sci*. 2012;53:5948–5954.

54. Ko MW, Leung LK, Lam DC, Leung CK. Characterization of corneal tangent modulus in vivo. *Acta Ophthalmol*. 2013;91:e263–e269.
55. Silverman RH, Lizzi FL, Ursea BG, et al. Safety levels for exposure of cornea and lens to very high-frequency ultrasound. *J Ultrasound Med*. 2001;20:979–986.
56. Ciuffreda KJ, Tannen B. Eye movement basics for the clinician. St. Louis, MO: Mosby; 1995.
57. Clayson K, Pavlatos E, Ma Y, Liu J. 3D characterization of corneal deformation using ultrasound speckle tracking. *J Innov Opt Health Sci*. 2017;10:174200–1742008.
58. Dias J, Ziebarth N. Impact of hydration media on ex vivo corneal elasticity measurements. *Eye Contact Lens*. 2015;41:281–286.
59. Rosenblat E, Hersh PS. Intraoperative corneal thickness change and clinical outcomes after corneal collagen crosslinking: standard crosslinking versus hypotonic riboflavin. *J Cataract Refract Surg*. 2016;42:596–605.
60. Vetter JM, Brueckner S, Tubic-Grozdanis M, Voßmerbaumer U, Pfeiffer N, Kurz S. Modulation of central corneal thickness by various riboflavin eyedrop compositions in porcine corneas. *J Cataract Refract Surg*. 2012;38:525–532.